

# Electronic structure of benzene adsorbed on single-domain Si(001)-(2 × 1): A combined experimental and theoretical study

S. Gokhale,<sup>a)</sup> P. Trischberger, D. Menzel, and W. Widdra<sup>b)</sup>  
*Physik-Department E20, Technische Universität München, D-85747 Garching, Germany*

H. Dröge and H.-P. Steinrück  
*Experimentelle Physik II, Universität Würzburg, 97074 Würzburg, Germany*

U. Birkenheuer,<sup>b)</sup> U. Gutdeutsch, and N. Rösch  
*Lehrstuhl für Theoretische Chemie, Technische Universität München, 85747 Garching, Germany*

(Received 20 October 1997; accepted 31 December 1997)

Benzene adsorption on a single-domain Si(001)-(2 × 1) surface has been studied by thermal desorption spectroscopy (TPD) and angle-resolved photoelectron spectroscopy (ARUPS) using linearly polarized synchrotron radiation. Angle-resolved photoemission spectra for the saturated benzene layer exhibit well-defined polarization and azimuthal dependencies compatible with a flat-lying benzene molecule with local  $C_{2v}$  symmetry. Based on these results two structure models are proposed. First-principles density functional cluster calculations have been performed for each of these structures. Total energy minimization and a detailed comparison of the experimental ARUPS spectra with the one-particle spectra of the model clusters leads to a 1,4-cyclohexadienelike adsorption complex with a flat-lying benzene molecule which is di- $\sigma$  bonded to the two dangling bonds of a single Si-Si surface dimer. Especially, one of the unoccupied  $1e_{2u}$  ( $\pi^*$ ) orbitals of the free benzene molecule shifts down (by about 3 eV) and evolves into the highest occupied molecular orbital (HOMO) of the chemisorbed molecule. © 1998 American Institute of Physics. [S0021-9606(98)03213-9]

## I. INTRODUCTION

The interactions of small unsaturated hydrocarbon molecules with silicon surfaces, especially with the technologically most important Si(001)-(2 × 1) surface, have been investigated in numerous experiments (e.g., Refs. 1–6) and computations (e.g., Refs. 6–10). Although details of the electronic structures are still under debate, the dominant bonding mechanism and the adsorption geometries seem to be understood. Studies on the interaction of *aromatic* hydrocarbons, on the other hand, are still rare. The adsorption of the highly symmetric benzene molecule on Si(001)-(2 × 1) has so far been the subject of just a single experimental study by Taguchi *et al.*<sup>11</sup> Only two theoretical investigations,<sup>12,13</sup> both based on semiempirical methods, have followed this initial experimental work.

The experimental study of benzene on Si(001)-(2 × 1)<sup>11</sup> was based on thermal desorption measurements (TPD), combined with Auger electron spectroscopy (AES), low energy electron diffraction (LEED), and high-resolution electron energy loss spectroscopy (HREELS). It was found that benzene chemisorbs nondissociatively with a saturation coverage of about 1/4 ML (defined as molecules per silicon surface atom). The analysis of the vibrational spectra revealed the presence of C=C double bonds and of both  $sp^3$  as well as

$sp^2$  hybridized carbon species, indicating the formation of  $\sigma$  bound cyclohexene- or cyclohexadienelike adsorption complexes. More specific details on the nature of the adsorption complex, however, could not be derived. The theoretical investigations, on the other hand, mainly focused on the geometrical structure of the adsorption complex. Different equilibrium configurations were found in both studies. Craig<sup>12</sup> proposed a tilted cyclohexenelike structure, fourfold bound to a single cleaved surface Si-Si dimer, whereas Jeong *et al.*<sup>13</sup> favored a slightly distorted  $C_{2v}$  symmetric, bi-radical structure, fourfold bound to two neighboring surface Si-Si dimers. More sophisticated, quantum chemical approaches have not been reported so far. Moreover, both studies report total energies only. A direct comparison of the corresponding electronic or vibrational structures with the experimental data is therefore not possible.

Due to this experimental and theoretical situation, one is still far from a detailed understanding of benzene adsorption on Si(001)-(2 × 1). Especially experimental data regarding its electronic structure and its symmetry are lacking. Here we present a detailed investigation of benzene adsorbed on Si(001)-(2 × 1) combining experimental data based on thermal desorption spectroscopy and angle-resolved UV (ultraviolet) photoelectron spectroscopy (ARUPS) with results from first-principles density functional (DF) calculations. As we will show, the electronic structure of the benzene molecule is substantially modified upon di- $\sigma$  bonding to this semiconductor surface. It therefore differs significantly from the one of benzene adsorbed on metal surfaces. Whereas the  $\sigma$  system of benzene is roughly maintained—though the

<sup>a)</sup>Permanent address: Dep. of Instr. Science, University of Pune, Pune 411 007, India.

<sup>b)</sup>Corresponding authors: E-mail: widdra@physik.tu-muenchen.de, Fax: x49-89-2891-2338, E-mail: birken@theochem.tu-muenchen.de, Fax: x49-89-2891-3622.

shape of participating orbitals is altered due to geometrical distortions (e.g., upward bending of the hydrogen atoms) and the inclusion of new Si–C bonds—the characteristic, delocalized aromatic  $\pi$  system of benzene is essentially destroyed during chemisorption and a completely new set of molecular orbitals emerges whose specific shapes strongly depend on the number and position of the Si–C bonds formed. A straightforward interpretation of the ARUPS data by means of photoemission spectra of gas-phase benzene is therefore hardly possible. In fact it will be shown, that the adsorption complex very much resembles a 1,4-cyclohexadiene molecule,  $C_6H_8$ , with two additional hydrogen atoms at diagonally opposite positions of the original benzene ring.

The organization of the paper is as follows: Details of the experimental measurements and the theoretical approach will be discussed in Secs. II and III. We then enter the analysis of the adsorption system by first presenting and discussing the experimental results (Secs. IV A and IV B). The results of the electronic structure calculations will be presented in the succeeding Secs. IV C and IV D, followed by the comparison of the experimental and theoretical spectra in Sec. IV E.

## II. EXPERIMENT

The experiments were performed in a two-chamber UHV system. It is equipped with a home-built multi-angle electron energy analyzer which allows—at a given azimuthal angle—the simultaneous detection of photoelectrons at polar angles between  $-10^\circ$  and  $90^\circ$  with respect to the surface normal.<sup>14</sup> The polar angular resolution is  $2^\circ$  and the azimuthal acceptance is  $3^\circ$ . For the ARUPS experiments linearly polarized light from the TGM-1 beamline at the Berlin synchrotron radiation facility (BESSY) was used. The energy resolution for the ARUPS spectra shown here was set to better than 200 meV. For additional characterizations, the chamber houses four grid LEED optics and a quadrupole mass spectrometer equipped with a Feulner cap.<sup>15</sup>

The experiments were performed on a single-domain Si(001)-(2 $\times$ 1) surface by using a Si(001) sample with a defined miscut angle of  $4.7^\circ$  towards the [110] direction (denoted as  $y$  axis in the following). By several cycles of sputtering and annealing to 1150 K followed by slow cooling (cooling rate  $-2$  K/s) well-ordered Si(001)-(2 $\times$ 1) terraces separated by double layer steps were prepared as indicated by a sharp single-domain (2 $\times$ 1) LEED pattern. The suppression of the  $90^\circ$  rotated minority domain was estimated to be better than 95% based on a quantitative analysis of ARUPS data for the clean surface. For homogeneous heating as well as cooling the silicon sample was bonded on a tantalum plate via a thin platinum and silver interlayer, which was evaporated on the back of the wet-chemical cleaned silicon wafer.<sup>16</sup> Using a liquid He cryostat, sample, and molybdenum plate could be cooled to 30 K and resistively heated to 1300 K. The temperature was measured indirectly by a chromel-alumel thermocouple on the backside of the molybdenum plate to avoid any contact of the (Ni-containing) thermocouple with the silicon sample. No significant temperature difference between silicon sample and thermocouple

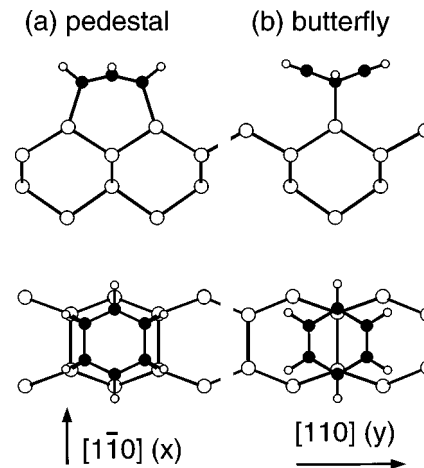


FIG. 1. The cluster models employed for the two  $C_{2v}$  symmetric structures of the adsorption complex  $C_6H_6/Si(001)$  shown in top view (lower panel) and along the silicon surface dimers (top panel): (a) Fourfold bound pedestal structure, (b) 1,4-cyclohexadiene-like butterfly structure. For simplicity the hydrogen atoms terminating the silicon cluster are omitted.

could be detected based on calibrations via desorption of rare gas and benzene multilayers<sup>17,18</sup> as well as of hydrogen.<sup>19</sup>

## III. COMPUTATIONAL DETAILS

It will be shown experimentally that benzene is adsorbed with its molecular plane parallel to the (001) surface of silicon with a local symmetry of  $C_{2v}$ . This casts serious doubts on tilted equilibrium structures like the one suggested in Ref. 12. For consistency with the experiment only  $C_{2v}$  symmetric models with flat-laying benzene molecules should be regarded, like the two cluster models considered here: A 1,4-cyclohexadienelike structure di- $\sigma$  bound to a single Si–Si dimer, and a bi-radical fourfold  $\sigma$  bound species, similar to the equilibrium configuration predicted in Ref. 13. The cluster models used to describe these adsorption complexes are shown in Fig. 1. They consist of the Si–Si dimers directly involved in the chemisorption and at least all nearest Si neighbors. Isolated dangling bonds are saturated by hydrogen atoms (not shown), and those dangling bonds pointing toward Si atoms which are multiply coordinated to the cluster already set up by silylene groups  $SiH_2$ . In the case of the 1,4-cyclohexadienelike (“butterfly”) structure [Fig. 1(b)], the cluster model is augmented by additional surface dimers to account for possible interactions with the hydrogen atoms of the adsorbed benzene molecule. The central surface dimer atoms and all adsorbate atoms are allowed to relax during the geometry optimization; all other substrate atoms are fixed to the corresponding bulk (or Si surface dimer) positions.

The density functional cluster calculations were performed with the LCGTO-DF (linear combinations of Gaussian-type orbitals—density functional) program<sup>20</sup> employing gradient-corrected exchange-correlation functionals<sup>21,22</sup> and state-of-the-art numerical integrations schemes.<sup>23,24</sup> Further details of these calculations and the basis sets employed—which have been proven to perform well on typical organo-silicon compounds such as  $SiH_4$  or the mixed carbon-silicon species  $H_3SiCH_3$ —can be found elsewhere.<sup>25</sup>

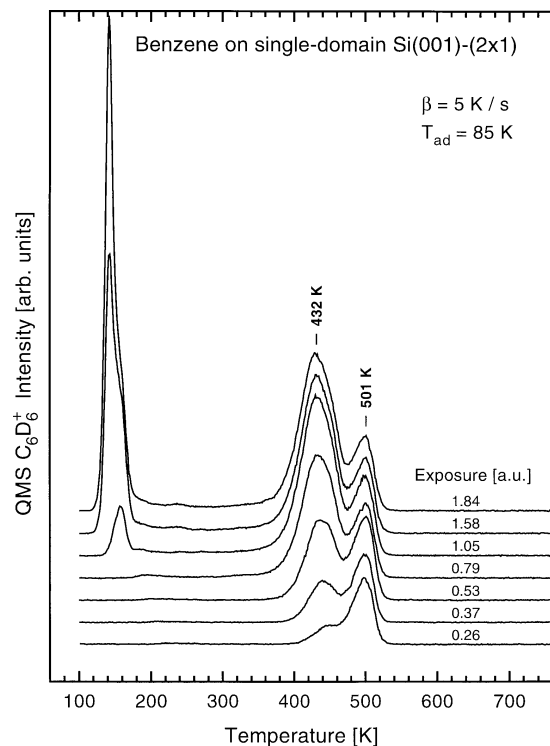


FIG. 2. Thermal desorption spectra for various exposures of deuterated benzene,  $C_6D_6$ , on a single-domain  $Si(001)-(2 \times 1)$  surface. The adsorption temperature was 85 K and a heating rate of 5 K/s was used.

## IV. RESULTS AND DISCUSSION

### A. Thermal desorption

Thermal desorption spectra after  $C_6D_6$  adsorption at 85 K on a single-domain  $Si(001)-(2 \times 1)$  surface are shown in Fig. 2. The spectra were recorded with a heating rate of 5 K/s and show the signal for mass 84 amu ( $C_6D_6^+$ ), the strongest line within the cracking products of deuterated molecular benzene. With increasing exposure three desorption peaks are observed. The high-temperature peak with a desorption maximum at 501 K saturates first. Subsequently, a second peak develops which shifts down in temperature from  $\sim 442$  to 432 K with increasing coverage. Both are due to molecular desorption of chemisorbed benzene. The exposures shown on the right in Fig. 2 are given relative to the exposure which saturates (at 85 K) the chemisorbed benzene layer. The high-temperature desorption peak at 501 K which is already close to saturation upon a relative exposure of 0.26 saturates at a coverage of 0.25 relative to the saturated chemisorbed benzene layer. It is attributed to benzene adsorption at or close to the double layer step edges separating the eight dimer wide (001) terraces of the vicinal crystal used.<sup>26</sup> Upon saturation of the step sites, adsorption on the terraces starts. The observed downward shift of its desorption temperature by 10 K might be due to repulsive interaction between the adsorbate molecules, most likely between neighboring molecules on different dimer rows. Higher exposures lead to desorption of physisorbed benzene layers. For the first physisorbed layer, as shown in Fig. 2, the desorption maximum shifts down from 155 to 140 K, which could be related to a slightly higher desorption energy for

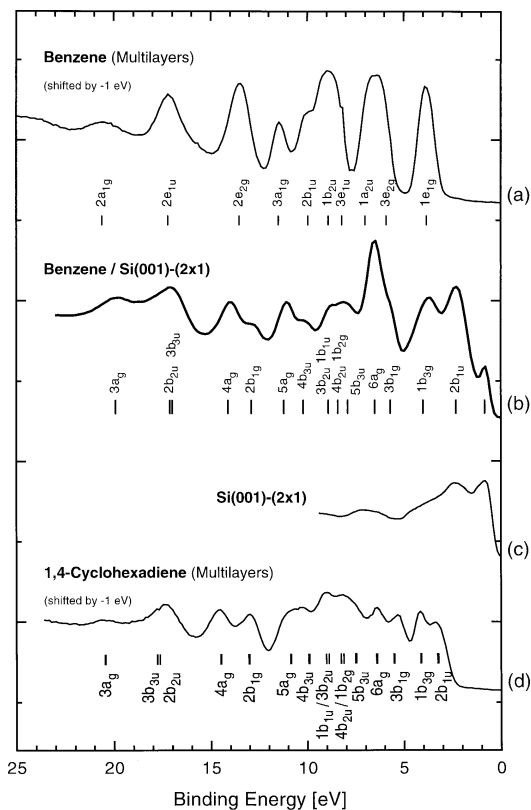


FIG. 3. UPS spectra for (a) condensed multilayers of benzene,  $C_6D_6$ , (b) benzene chemisorbed on  $Si(001)-(2 \times 1)$ , and (d) for condensed multilayers of 1,4-cyclohexadiene,  $C_6H_8$ . For comparison a spectrum for the clean surface under identical conditions is shown in (c). A photon energy of 50 eV at normal light incidence was used. The multilayer spectra have been shifted by about 1 eV to align the lowest lying photoemission features. The assignments of the multilayer 1,4-cyclohexadiene spectrum shown at the bottom result from a DF calculation on the gas-phase molecule. To improve agreement with experiment the Kohn–Sham one-particle spectrum has been shifted by 2.8 eV and scaled with a factor of 1.15.

second layer benzene close to the steps. Besides desorption of molecular benzene as shown here, no desorption of decomposition products (e.g., no  $D_2$  desorption which would be expected to desorb around 800 K) was observed for any exposure. This indicates that benzene desorption on  $Si(001)$  is *completely* molecular. Additional TPD experiments, not shown here, for  $C_6D_6$  adsorption on a partially H-covered  $Si(001)-(2 \times 1)$  surface show again completely molecular  $C_6D_6$  desorption without isotopic exchange. This proves that the benzene C–D bonds stay intact upon adsorption and thermal activation up to the desorption temperature. Whereas molecular benzene desorption from metal surfaces is mostly observed for higher coverages only due to site blocking for the decompositions products, benzene desorption on  $Si(001)$  is completely molecular for all coverages. The high desorption temperature (up to 500 K as shown in Fig. 2) points to stronger benzene–silicon interactions than typical for benzene–metal systems which exhibit molecular benzene desorption.

### B. Angle-resolved photoemission

In Fig. 3 photoemission data of the valence band region for a saturated benzene layer chemisorbed on  $Si(001)-$

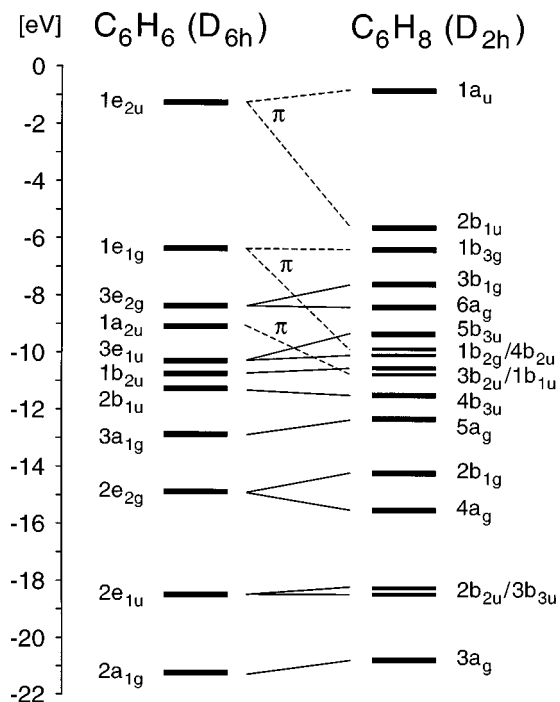


FIG. 4. Correlation diagram between the Kohn–Sham one-particle levels of gas-phase benzene and gas-phase 1,4-cyclohexadiene evaluated at the corresponding DF equilibrium geometries. Solid lines connect orbitals which are symmetric with respect to the plane of the carbon atoms, dashed lines connect orbitals which are anti-symmetric (the  $\pi$  system of benzene). HOMO of benzene:  $1e_{1g}$ , HOMO of 1,4-cyclohexadiene:  $2b_{1u}$ .

( $2 \times 1$ ) are compared to UPS (ultraviolet photoelectron spectroscopy) spectra of condensed benzene multilayers (top) and of condensed 1,4-cyclohexadiene multilayers (bottom). For comparison a spectrum for the clean surface is given in Fig. 3(c) as well. All four spectra were recorded with a photon energy of 50 eV. The multilayer spectra have been down shifted by about 1 eV to align the lowest levels,  $3a_g$  and  $2a_{1g}$ , respectively. The well-established assignment of the photoemission features of condensed benzene, as labeled in Fig. 3(a),<sup>27</sup> is taken from a comparison with gas-phase spectra.<sup>28</sup> The comparison of the spectra for condensed and chemisorbed benzene reveals significant differences. Besides an additional peak in Fig. 3(b) at  $\sim 1.2$  eV which is attributed to the silicon dangling bond state, the benzene-derived features show splitting of degenerate orbitals, best visible for the  $2e_{2g}$  and the  $1e_{1g}$  orbitals, as well as drastic shifts in energy. As already mentioned, we will show that the electronic structure of the di- $\sigma$  bonded benzene molecule resembles more closely the electronic structure of 1,4-cyclohexadiene,  $C_6H_8$ . Consequently and to avoid unnecessary relabeling, we will use the nomenclature of the 1,4-cyclohexadiene molecule, which in the gas phase has  $D_{2h}$  symmetry, to identify the orbitals of chemisorbed benzene in the following. To illustrate the similarities of the electronic spectra for chemisorbed benzene and 1,4-cyclohexadiene, the UPS spectrum for condensed multilayers of 1,4-cyclohexadiene molecules is shown in Fig. 3(d). The orbital energies resulting from our DF calculation on gas-phase 1,4-cyclohexadiene molecule are indicated as bars below the spectrum in Fig. 3(d). The agreement is good and the

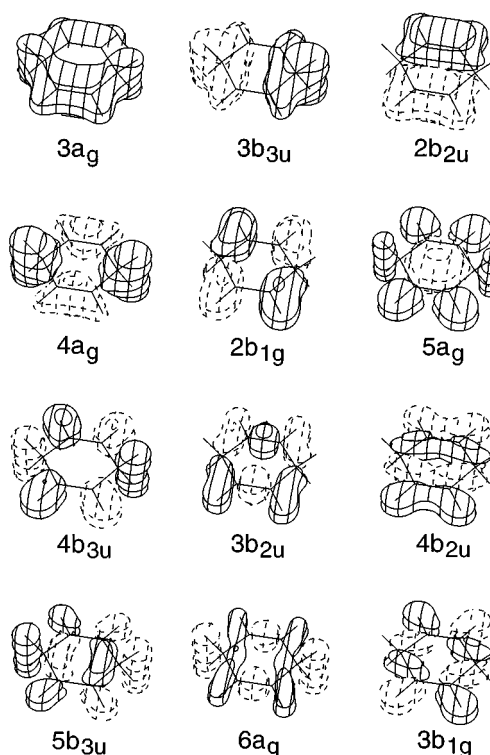


FIG. 5. Sketch of those occupied orbitals of gas-phase 1,4-cyclohexadiene which are symmetric with respect to the molecular plane and thus related to the  $\sigma$  system of benzene.

orbital assignment for condensed 1,4-cyclohexadiene therefore straightforward. Returning to the interpretation of the angle-integrated UPS spectrum of benzene on the Si(001) surface, we first note that the splitting of the former benzene  $2e_{2g}$  orbital into the  $4a_g$  and  $2b_{1g}$  orbitals can be seen easily. A detailed analysis will show that the splitting of the symmetry-equivalent former benzene  $3e_{2g}$  orbitals into the  $6a_g$  and  $3b_{1g}$  orbitals is similar for 1,4-cyclohexadiene and  $C_6D_6$  on Si(001) as well. The two observed photoemission features at 4.0 and 2.3 eV correspond to the two highest occupied molecular orbitals (HOMOs),  $1b_{3g}$  and  $2b_{1u}$ , of 1,4-cyclohexadiene and are not—as one might speculate—the splitting product of the degenerate benzene  $1e_{1g}$  state. For a direct comparison of the corresponding benzene and 1,4-cyclohexadiene molecular orbitals and their energetical differences we refer to the orbital correlation diagram in Fig. 4, which results from DF calculations on gas-phase benzene and gas-phase 1,4-cyclohexadiene. The splitting of the degenerate benzene orbitals upon symmetry reduction from  $D_{6h}$  to  $D_{2h}$  and the down-shift of one of the former unoccupied benzene  $\pi^*$  orbitals ( $1e_{2u}$ ) which becomes occupied in 1,4-cyclohexadiene due to the additional electrons from the added H atoms are the dominant changes. Note however, that the differential shifts found for 1,4-cyclohexadiene might be quite different from those for  $C_6D_6$  on Si(001) because of the different chemical nature of the silicon substrate compared to the hydrogen atoms, and due to the additional interaction channels which open upon reduction of the symmetry to  $C_{2v}$  or even less. The shape of the new 1,4-cyclohexadiene orbitals are depicted in Figs. 5 and 6. Comparison to the well-

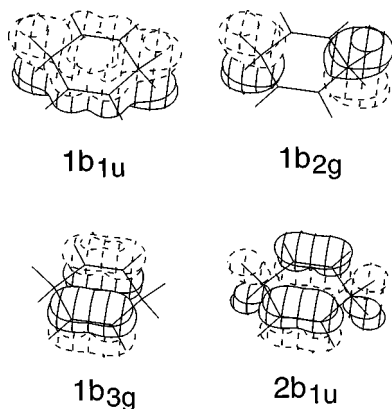


FIG. 6. Sketch of those occupied orbitals of gas-phase 1,4-cyclohexadiene which are anti-symmetric with respect to the molecular plane and thus related to the  $\pi$  system of benzene.

known molecular orbitals of benzene<sup>29</sup> reveals that the orbitals which are symmetric with respect to the molecular plane of  $C_6H_8$  (defined by the C atoms) are quite similar to the  $\sigma$  orbitals of benzene (Fig. 5), whereas the anti-symmetric  $C_6H_8$  orbitals shown in Fig. 6 differ substantially from the characteristic  $\pi$  system of benzene. The  $C_6$  symmetric  $\pi$  orbital of benzene is essentially preserved as  $1b_{1u}$  orbital in 1,4-cyclohexadiene; all other benzene  $\pi$  features are lost. Most typical for 1,4-cyclohexadiene are the orbitals  $1b_{3g}$  and  $2b_{1u}$  which are dominantly made up by the symmetric

and anti-symmetric linear combinations of the two  $\pi$  orbitals attributed to the  $C=C$  double bonds on the opposite sides of the carbon ring.

To illuminate the electronic structure of benzene chemisorbed on Si(001)-(2 $\times$ 1) in more detail, angle-resolved photoelectron spectroscopy with different photon energies in the range of 25–50 eV was employed using a single-domain prepared Si(001)-(2 $\times$ 1) surface. Benzene layers of different coverages have been investigated; here we show data for the saturated benzene layer which have been well-reproduced on three different single-domain Si(001)-(2 $\times$ 1) crystals. Photoemission data for lower benzene coverages and adsorption at step sites will be presented elsewhere.<sup>26</sup> The angle-resolved photoemission spectra of a saturated benzene layer for polar emission angles from 0 to 70° using normal incident light with a photon energy of 50 eV are depicted in Fig. 7. The spectra are displayed for four different experimental geometries concerning the light polarization (denoted as  $E_x$  and  $E_y$ ) as well as the azimuthal photoelectron detection plane (noted as  $D_x$  and  $D_y$ ) with respect to the high symmetry directions, [110] and  $[\bar{1}\bar{1}0]$ , of the Si(001) substrate as indicated in Fig. 8. In the binding energy range from 25 to 5 eV ten photoemission features can be observed which are all attributed to benzene-derived molecular orbitals. Additionally there are three strong features in the range of 5–0 eV which are attributed to the two highest occupied molecular orbitals of the adsorption complex at 4.0 and 2.3 eV and to a

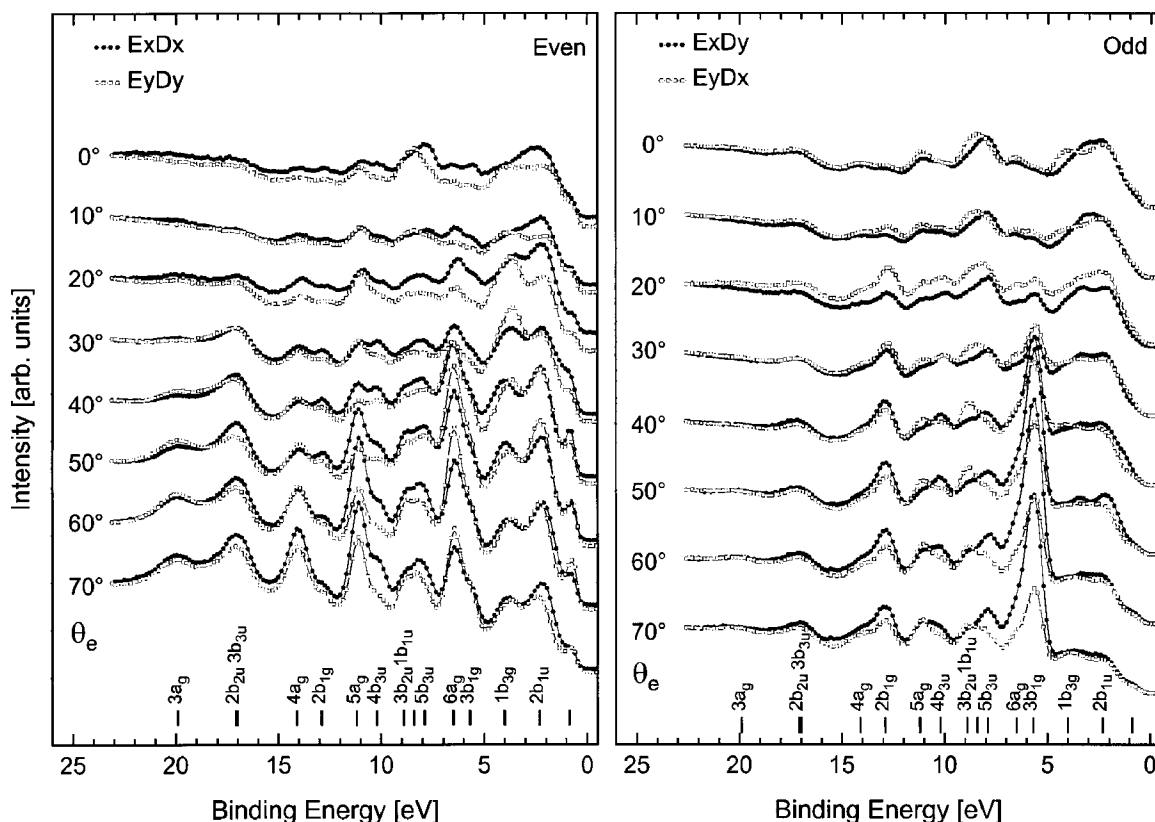


FIG. 7. ARUP spectra for the saturated benzene layer on a single-domain Si(001)-(2 $\times$ 1) surface at normal light incidence for a photon energy of 50 eV. Spectra for light polarization and photoelectron detection plane both in the [110] and the  $[\bar{1}\bar{1}0]$  azimuths, indicated as  $E_xD_x$  and  $E_yD_y$ , respectively, are depicted on the left. Spectra with the photoelectron detection plane perpendicular to the light polarization, indicated as  $E_xD_y$  and  $E_yD_x$ , are shown on the right.

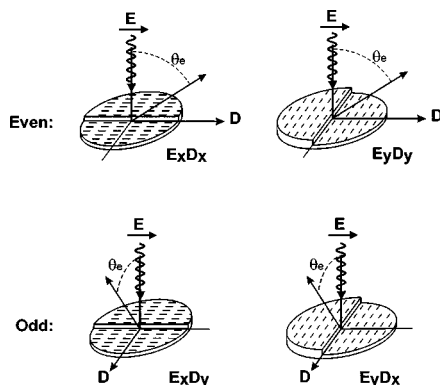


FIG. 8. Schematic illustrations of the four experimental geometries used for the angle-resolved photoemission on the single-domain Si(001)-(2 $\times$ 1) surface. The light polarization vector is indicated by  $E$  and the azimuthal photoelectron detection plane by  $D$ .

remaining silicon dangling bond state at 0.85 eV. Photoemission from the 12 eV wide silicon  $sp$  band is rather weak. Some of the substrate-related features, such as dimer, back bond, and dangling bond states, are visible in the range 5–1 eV for experimental conditions where the benzene-derived features are weaker. None of the benzene-derived orbitals exhibit any dispersion (within  $\pm 0.1$  eV) for the saturated layer indicating negligible lateral interactions. For the assignment of the ARUPS features we start with the peak of highest binding energy at 19.9 eV. It is attributed to the  $3a_g$  orbital of a 1,4-cyclohexadienelike adsorption complex which corresponds to the  $2a_{1g}$  orbital of the free benzene molecule. At normal light incidence as is shown in Fig. 7, this peak is only visible in the even geometries ( $E_x D_x$  and  $E_y D_y$ ) and for non-normal electron emission as is expected for benzene adsorption in the highest possible  $C_{2v}$  symmetry. The peak at a binding energy of 17.1 eV which is derived from the former degenerate  $2e_{1u}$  benzene orbital is assigned to the  $2b_{2u}$  and  $3b_{3u}$  states. The possible splitting into states which belong to the  $b_1$  and  $b_2$  representations of  $C_{2v}$  symmetry for a flat-lying benzene structure is difficult to detect, as in the case of condensed 1,4-cyclohexadiene. Closer inspection shows a slight broadening on the energetically lower side (higher binding energy) for the  $E_y$  geometries compared to the  $E_x$  geometries which might indicate a slightly lower energy for the  $b_2$ -type orbital. For a possible “vertical” benzene structure with  $C_{2v}$  symmetry in which the molecular ring is oriented perpendicular to the surface and aligned along the surface dimer (the  $x$  axis), a splitting of the  $2e_{1u}$  orbitals into  $a_1$  and  $b_1$  states is predicted. Based on dipole selection rules, this would lead to forbidden photoemission in the odd  $E_y D_x$  geometry. Instead, these states are observed equally well in both odd geometries,  $E_y D_x$  and  $E_x D_y$ , see Fig. 7(b). Therefore we rule out such a vertical adsorption geometry.

The two adjacent peaks at 14.1 and 12.9 eV show strong complementary emission characteristics. The former is only visible in even geometries ( $E_x D_x$  and  $E_y D_y$ ) whereas the latter shows strong emission in odd geometries ( $E_x D_y$  and  $E_y D_x$ ) only. These peaks are attributed to the  $4a_g$  ( $a_1$ ) and  $2b_{1g}$  ( $a_2$ ) molecular orbitals, respectively. This corresponds

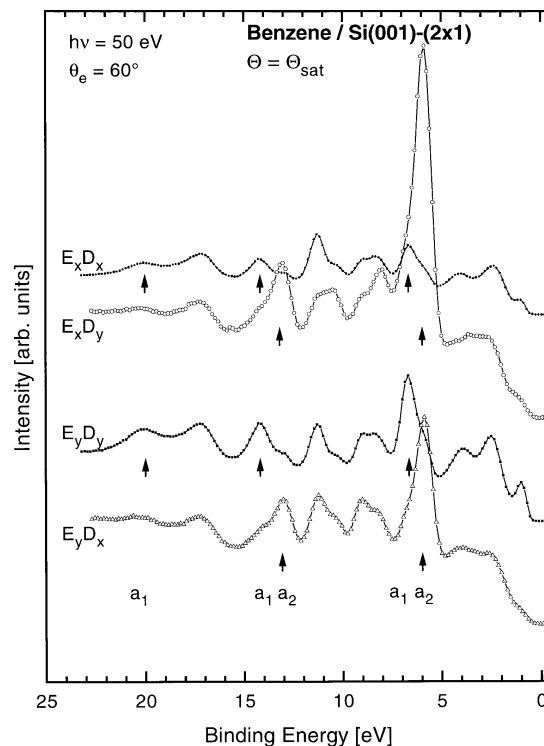


FIG. 9. ARUPS spectra for the saturated benzene layer on a single-domain Si(001)-(2 $\times$ 1) surface at a fixed emission angle of  $60^\circ$  and normal light incidence ( $h\nu=50$  eV). Different light polarizations and detector orientations are marked on the left. The complementary emission characteristics of states of  $a_1$  and  $a_2$  symmetry are indicated by arrows.

to a 1.2 eV splitting of the gas-phase benzene  $2e_{2g}$  orbital which is similar to the splitting in gas-phase 1,4-cyclohexadiene. Additionally, we recognize a small but non-vanishing emission of the  $2b_{1g}$  orbital in some  $E_x D_x$  spectra which is forbidden for a strict  $C_{2v}$  symmetry and seems to indicate a broken adsorbate  $xz$  mirror plane. This deviation from  $C_{2v}$  symmetry will be discussed in detail below. For the alternative vertical benzene structure, one would expect a different splitting of the former benzene  $2e_{2g}$  molecular orbital into states which belong to the  $a_1$  and  $b_1$  representations. Again, the observed strong emission in both odd geometries for the higher lying state at 12.9 eV clearly rules out this proposition. The benzene-derived molecular orbitals in the 11.2–2.3 eV range fall into the silicon  $sp$  band and, therefore, might interact with silicon surface states, surface resonances, or bulk states. Here we start by correlating the dominant photoemission features to the corresponding gas-phase molecular orbitals. The differential shifts due to the adsorbate-substrate interaction will be addressed in the following theory section. The dominant photoemission features at 6.5 and 5.7 eV show again strong complementary emission characteristics and, based on their symmetry characters, they are attributed to the former degenerate  $3e_{2g}$  benzene orbitals. The peak at 6.5 eV features emission under non-normal even geometries and thus is assigned to the  $6a_g$  ( $a_1$ ) orbital; the peak at 5.7 eV which shows significant emission under non-normal odd geometries corresponds to the  $3b_{1g}$  ( $a_2$ ) molecular orbital. To demonstrate these distinct azimuthal dependencies, photoemission spectra for a constant

polar angle of  $60^\circ$  are depicted in Fig. 9. The splitting of the degenerate benzene  $2e_{2g}$  and  $3e_{2g}$  orbitals into pairs of states with  $a_1$  and  $a_2$  symmetry each is marked by arrows.

By comparison to the spectra of condensed 1,4-cyclohexadiene, the high-energy peaks at 4.0 and 2.3 eV are assigned to the  $1b_{3g}$  ( $b_2$ ) and  $2b_{1u}$  ( $a_1$ ) orbitals (the HOMOs of 1,4-cyclohexadiene), respectively. They therefore are related to the anti-symmetric and symmetric linear combination of the two occupied C=C  $\pi$  orbitals of the adsorption complex (see Fig. 6), an assignment which is confirmed by our first-principles calculations. The totally symmetric  $\pi$  orbital  $2b_{1u}$  can clearly be seen in even geometries. Similar emission in even geometry is discernible for the  $1b_{3g}$  state whose energy (between 3.7 and 4.0 eV) seems to depend on the emission angle as well as on the experimental geometry,  $E_x D_x$  versus  $E_y D_y$  [see Fig. 7(a)]. However,  $C_{2v}$  based dipole selection rules appear to be violated for this assignment: The  $2b_{1u}$  state apparently shows intensity in the odd geometries which is not allowed for an  $a_1$ -type orbital and the  $1b_{3g}$  state seems to show equal intensity in both even geometries although this emission is forbidden for  $E_x D_x$ . On the other hand, the situation is complicated experimentally by the fact that photoemission from silicon-derived states also contributes significantly in this energy range: One has to bear in mind that on the clean surface the  $D_i$  surface resonance<sup>30</sup> dominantly related to the Si–Si dimer bond, is located in the range between 2 and 3 eV as shown by photoemission data for the clean Si(001)-(2 $\times$ 1) surface.<sup>31</sup> Additionally, photoemission in the odd geometries is expected in this range due to substrate and back bond emission, for instance the  $B_1$  back bond state<sup>30</sup> which under our experimental conditions shows strong emission (at about 2 eV) in the  $E_x D_y$  geometry on the clean Si(001)-(2 $\times$ 1) surface.<sup>31</sup> In the region around 4.0 eV, where the  $B_3$ ,  $B_4$ , and  $B_5$  back bond states have been predicted for the clean surface,<sup>30</sup> the clean Si(001)-(2 $\times$ 1) surface shows structures as well.<sup>31</sup> Based on these considerations, the emission in the odd geometries at 2–2.3 eV might be due to the  $B_1$  back bond state and not to the  $2b_{1u}$  state which is supported by the slightly different energy position in the even and odd spectra (Fig. 7). The energy shift with emission angle of the peak attributed to the  $1b_{3g}$  state, best visible for a polar angle of  $40^\circ$ , might either be due to lateral interaction and the resulting dispersion of this state or to contributions from a second photoemission peak close by which exhibits angle-dependent intensity. The lack of any periodicity of the observed shifts with  $k_{\parallel}$  rules out real dispersion. This is expected since the benzene–benzene distance along the Si–Si dimer row amounts to 7.7 Å (twice the dimer–dimer distance) which is significantly larger than the van der Waals diameter of benzene (6.7 Å<sup>32</sup>) or the distance for which dispersion has been observed on metal surfaces, e.g., 6.6 Å on Ni(110).<sup>33</sup> Substantial direct orbital overlap can therefore be excluded. Thus, we attribute this emission in  $E_x D_x$  geometry, which is stronger than on the clean surface, to either a modified bulk/back bond emission or to the  $D_i$  surface resonance (an  $a_1$  state) down-shifted upon interaction with the totally symmetric  $\pi$  orbital  $2b_{1u}$ .

The four photoemission peaks at 11.2, 10.2, 8.9, 8.4, and 7.9 eV are tentatively assigned to the seven remaining mo-

lecular orbitals: The  $5a_g$ ,  $4b_{3u}$ ,  $1b_{1u}+3b_{2u}$ ,  $4b_{2u}+1b_{2g}$ , and  $5b_{3u}$  states, respectively. The weak peak at 8.4 eV is hardly visible in Fig. 7 but can be identified more clearly at lower photon energies. This energy sequence corresponds to that found for condensed 1,4-cyclohexadiene (see Fig. 3), and agrees reasonably with the observed symmetry characters of the photoemission features. However, since several peaks overlap the assignment is tentative only and further theoretical support is required.

In addition to the benzene-derived features discussed above, photoemission intensity at a binding energy of about 0.8 eV, close to the top of the silicon valence band, can be seen in the ARUPS spectra for even geometry ( $E_x D_x$  and  $E_y D_y$ , see Fig. 7). This peak is attributed to the remaining dangling bond states,  $D_{up}$ , on those Si–Si dimers where no benzene molecules are chemisorbed. No dispersion of this dangling bond state is visible in the spectra, which, on the other hand, amounts to 0.5–0.8 eV along the dimer rows on the clean Si(001)-(2 $\times$ 1) substrate.<sup>31,34</sup> Again the absence of dispersion is expected since benzene adsorption (at saturation coverage) takes place on every second Si–Si dimer due to steric hindrance and therefore prevents any significant interaction of the remaining dangling bonds along the dimer rows.

As demonstrated in the given detailed analysis, the ARUPS spectra can be successfully assigned based on a cyclohexadienelike di- $\sigma$  bonded structure. We have started the analysis with the highest possible symmetry of the adsorption complex,  $C_{2v}$ , and found deviations which may be rationalized by a lower  $C_s(yz)$  adsorption symmetry (broken  $xz$  mirror plane, see Fig. 1). On the other hand, as we have seen, thermal desorption shows two distinct desorption peaks which have been attributed to desorption from terraces and step sites, respectively. Therefore, one possible explanation for the observed intensity in forbidden geometries might be a superposition of photoemission from adsorbates with different orientations or local symmetry due to adsorption on the terrace and at the step site. However, it is possible to prepare both benzene species separately and to analyze their angle-resolved photoemission spectra separately. As we will show elsewhere,<sup>26</sup> ARUPS spectra for benzene adsorption at double layer step sites indicate that these step species are also oriented in highly symmetric fashion and thus cannot account for the observed deviation from  $C_{2v}$  symmetry.

An alternative, straightforward explanation is linked to the vicinal Si(001) crystal used. To obtain a single-domain (2 $\times$ 1) surface by preparing (001) terraces separated by double layer steps, a sample with 4.7° miscut towards the [110] direction was used. Hence the *macroscopic* surface normal deviates from the surface normal of the local (001) terraces. This has three consequences for a detailed analysis of high-quality ARUPS spectra (with good signal to noise ratios): (i) Since  $k_{\parallel}$  is only conserved with respect to the macroscopic surface—according to its 30 Å translational symmetry—the macroscopic normal was used in the present study to align the crystal (defining the  $z$  axis). Thus, normal emission ( $k_{\parallel}=0$ ) here refers to the origin of the large surface Brillouin zone of the *vicinal* crystal with terraces of eight dimers width separated by double layer steps. The local sym-

metry observed in the photoemission spectra, however, has been discussed with reference to the local  $C_{2v}$  ( $2 \times 1$ ) terrace structure. Emission with a vanishing  $y$  component of the electron momentum therefore locally corresponds to emission with  $k_y = 0.51 \text{ \AA}^{-1} \sin(4.7^\circ) \sqrt{E_{\text{kin}}/\text{eV}}$ . Hence, one has to be careful when analyzing normal emission data for a vicinal crystal. Furthermore, due to the offset in  $k_y$ , the  $x$  direction is no longer a high symmetry direction. Strictly, the symmetry of the surface is reduced to  $C_s(yz)$  due to the terrace-step sequence and the highest possible adsorption symmetry therefore can only be  $C_s(yz)$ . (ii) For *macroscopic* normal light incidence the light has a component of about 8% polarized in the local (terrace)  $z$  direction. This may lead to dipole transitions which would be forbidden for perfect in-plane polarization. (iii) In addition to the steps along the  $y$  direction, the dimer rows are shifted from terrace to terrace by a quarter unit cell in  $x$  direction which results in a non-rectangular primitive unit cell (deviation  $3.4^\circ$ ). High kinetic-energy photoemission along the  $x$  direction (high  $k_x$  values, e.g., located in the second or third Brillouin zone) leads to deviations from high-symmetry final states due to this  $3.4^\circ$  deviation. Summarizing one can therefore state that the selection rules observed in the photoemission spectra may be fully compatible with a local  $C_{2v}$  symmetric adsorption complex; deviations are solely due to the reduced surface symmetry arising from the intentional sample miscut, necessary to suppress the other domain.

### C. Structure optimization

To determine the binding energy for the proposed structures shown in Fig. 1, geometry optimizations have been performed for both, the model clusters of the adsorption complex and the corresponding substrate clusters  $\text{Si}_{15}\text{H}_{16}$  and  $\text{Si}_{13}\text{H}_{12}$  prior to benzene adsorption. Except for the ‘‘pedestal’’ adsorption complex, Fig. 1(a), all calculations were performed spin-restricted. The pedestal structure, on the other hand, is an open shell system with dangling bonds on each of the threefold coordinated carbon atoms and thus has been treated in spin-polarized fashion. The open shell configuration is confirmed by our DF calculations: The HOMO and LUMO (lowest unoccupied molecular orbital) of the model cluster essentially consist of the symmetric and anti-symmetric linear combinations of the  $p_z$  orbitals on the two carbon atoms not participating in the bonding toward the substrate, and only a small energetic splitting of these states (less than 0.2 eV) was found indicating little spatial overlap of the two local orbitals involved.

The binding energies are computed to 1.40 and 0.15 eV for the butterfly and the pedestal structure, respectively. Thus according to our DF cluster calculations the 1,4-cyclohexadienelike structure is energetically favored. On the other hand, total energy minimization of the same model clusters by means of a semiempirical method [modified neglect of differential overlap (MNDO/ $d$ )]<sup>25</sup> resulted in the opposite preference. Fourfold bound benzene species are favored by other semiempirical methods as well.<sup>12,13</sup> One may speculate that semiempirical approaches in general somewhat overestimate the strength of the Si–C bonds in the

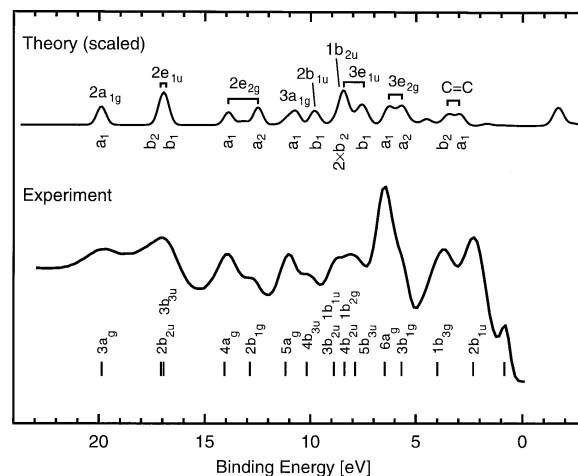


FIG. 10. Comparison of the experimental photoemission spectra of benzene adsorbed on Si(001) (bottom) with the adsorbate projected density of states (PDOS) of the model cluster for the butterfly structure of the adsorption complex. The  $C_{2v}$  symmetry character of the dominant contribution to the PDOS are given underneath, the benzene orbitals to which these features are related are indicated above the simulated spectrum. The symmetry labels of the photoemission spectrum are as in Fig. 3.

present, rather substantially distorted adsorption complex  $\text{C}_6\text{H}_6/\text{Si}(001)$  and therefore exhibit an unrealistic preference for fourfold bound species. However, in this combined experimental and theoretical study we do not rely solely on binding energies to discriminate between the two structure models. Calculation of the symmetry-resolved electronic structure for the different models and direct comparison with the experimental angle-resolved photoemission spectra will provide further information on the geometry of the adsorption system and evidence for the 1,4-cyclohexadienelike butterfly adsorption structure.

Before turning to these simulations, we would like to mention a few interesting features of the equilibrium structure found in the DF cluster calculations. The length of the C=C double bonds in the 1,4-cyclohexadienelike butterfly structure of the adsorption complex [Fig. 1(b)] is contracted by 0.05  $\text{\AA}$  while that of the remaining C–C single bonds is elongated by 0.11  $\text{\AA}$  with respect to gas-phase benzene (calc. to 1.40  $\text{\AA}$ ). Moreover the bond angles at the carbon atoms not involved in the Si–C bonds amount to  $120^\circ \pm 1.5^\circ$ , while those at the fourfold coordinated carbon atoms are close to the ideal tetrahedron angle, both indicating almost perfect  $sp^2$  and  $sp^3$  hybridization, respectively, within the benzene molecule after chemisorption at the Si(001) surface. The explicit structural parameters are extensively discussed elsewhere.<sup>25</sup>

### D. One-particle energy spectra

Rigorously, Kohn–Sham one-particle energies are not related to photoionization energies. Yet they provide useful information for a qualitative and even a semiquantitative interpretation of photoemission (and inverse photoemission) spectra, as has been demonstrated in a series of applications to the adsorption of hydrocarbons on transition metals.<sup>35–37</sup> There is, however, one major difference between the adsorption of organic molecules on transition metals studied so far

and their adsorption on silicon. In the former case the energies of almost all occupied molecular valence orbitals happen to fall below the valence band of the metallic substrate, and hence in the energy range of interest the electronic structures of the two sub-systems are to a large degree decoupled. In case of silicon, on the other hand, the most important occupied orbitals of the adsorbate turn out to coincide energetically with the valence band of the semiconductor. Actually, the valence band of silicon extends over more than 12 eV (from 16.0 to 1.5 eV for the  $\text{Si}_{15}\text{H}_{16}$  cluster) and only the first three (out of 15) valence orbitals of benzene, the  $2a_{1g}$  and the twofold degenerate  $2e_{1u}$  ones, are lower in energy than the substrate valence band (see Fig. 10).

As a consequence, the common two-level orbital interaction scheme, often serving as guidance for the interpretation of adsorption induced level shifts, can no longer be applied. Instead of essentially forming one bonding and one anti-bonding linear combination, the individual molecular orbitals can now interact with a continuum of substrate states. This results in adsorbate involved re-hybridizations which are spread over many orbitals of the adsorption system, most of them containing so little adsorbate admixtures that their contributions to the photoemission signal are usually hidden in the essentially featureless background intensity. Only electrons from well-localized surface states (with energies in the band gap) or from resonance-like states with a high localization at the surface (with energies that fall into the valence band) have a significant chance to yield prominent features in the photoemission spectra. Following this line of reasoning we will try to interpret the photoemission spectra recorded for benzene on Si(001) by associating the ARUPS peaks with those orbitals of the model clusters  $\text{C}_6\text{H}_6/\text{Si}_{13}\text{H}_{12}$  and  $\text{C}_6\text{H}_6/\text{Si}_{15}\text{H}_{16}$  which exhibit an enhanced probability amplitude within the adsorbate and the first surface layers. In the present investigation the localization of the wave functions is measured by the Mulliken populations on the adsorbate. Populations from the first substrate surface layer could have been considered as well, but because of the general ambiguity of a Mulliken population analysis it would have been hard to properly separate Si back bond contributions from contributions that we are aiming at: The Si-C and the Si-Si dimer bonds.

In the upper panel of Fig. 10, the density of states of the model cluster for the butterfly structure projected on the adsorbate is shown. The labels underneath the curve indicate the symmetry character of the dominant contributions to each feature of the projected density of states (PDOS) as obtained from a symmetry-resolved projection analysis and from inspection of the cluster orbitals involved. These symmetry labels are directly comparable to the results of the dipole selection rule analysis of the corresponding photoemission signals (see Sec. IV E). The double peak in the PDOS at about 4 eV is due to the symmetric ( $a_1$ ) and anti-symmetric ( $b_2$ ) linear combination of the two  $\pi$ -type orbitals of the adsorption complex which describe the C=C double bonds of the adsorbate. All other features of the simulated spectrum turn out to be exclusively related to  $\sigma$ -type orbitals. Neither the  $1b_{1u}$  nor the  $1b_{2g}$  derived  $\pi$ -type orbitals (see Fig. 6) show up distinctively in the projected density of

states. A detailed population analysis reveals that admixtures of these two orbitals are scattered over many cluster states with minor adsorbate contributions only in each of them. Following this reasoning, no further photoemission peaks related to the remnants of the benzene  $\pi$  system should be discernible in the photoemission spectrum (see also discussion in Sec. IV E). However, one has to take into account that only the benzene contributions to the density of states is analyzed here. Photoemission features arising from surface feature which are dominantly localized within the surface layers of the substrate (such as the back bond states of the clean Si(001) surface which indeed are visible in photoemission spectra) are not well represented by the PDOS shown in Fig. 10. Thus it can not completely be excluded that some of the former adsorbate  $\pi$  orbitals significantly participate in such sub-adsorbate layer features. The cluster models employed are too small to extract any definite statement about this possibility.

For the  $\sigma$  system the situation is completely different. Upon chemisorption the  $\sigma$  orbitals of the adsorbate are altered far less (as was the case when passing from benzene to 1,4-cyclohexadiene) and thus there exists an almost perfect one-to-one correspondence between the original benzene  $\sigma$  orbitals, the gas-phase 1,4-cyclohexadiene orbitals (shown in Fig. 5) and corresponding states of the model cluster. Each of these cluster states is rather localized on the adsorbate and therefore gives rise to a sharp peak in the projected density of states. This one-to-one correspondence is indicated by the upper labels of the PDOS curve in Fig. 10. At first glance such a relation is somewhat unexpected, especially in the light of a recent investigation on the adsorption of ethylene on Si(001).<sup>6</sup> There indeed, only few of the ethylene  $\sigma$  states end up in strong surface resonances after chemisorption. However, a closer analysis of the shape of the orbitals reveals that for the adsorption system  $\text{C}_6\text{H}_6/\text{Si}(001)$  all of the benzene  $\sigma$  orbitals which, from the energetic point, are able to interact with the valence band of the silicon substrate (from  $3a_{1g}$  up to  $3e_{2g}$ ) accidentally happen to have a nodal plane (or only a small amplitude in case of the  $2b_{1u}$  orbital) in the direction of the Si-C bonds. This very efficiently suppresses any direct overlap between the adsorbate and the substrate orbitals which would be required for a strong coupling and the concomitant broadening of the surface resonances. Hence, to some extent, it is happenstance that *all* of the benzene  $\sigma$  orbitals evolve into localized surface states or resonances upon chemisorption on Si(001).

Judging from the analysis of the electronic structure of the butterfly structure model, very similar photoemission characteristics are expected for the pedestal structure in the energy range below 5 eV. Yet in the comparative investigation of the two different structure models some noteworthy differences were found.<sup>25</sup> The order of the symmetry character of the split benzene  $2e_{2g}$  and  $3e_{2g}$  orbitals is different for the two structure models. In case of the butterfly structure the  $a_1$  symmetric partner of the  $2e_{2g}$  orbital, the 1,4-cyclohexadiene  $4a_g$ -derived one, is lower in energy than the  $a_2$  symmetric partner which evolves into the  $2b_{1g}$  state of the 1,4-cyclohexadienelike adsorption complex (see Fig. 10). In a similar way the  $3e_{2g}$  state of benzene splits into the

1,4-cyclohexadiene  $6a_g$  and  $3b_{1g}$  derived orbitals, with the former totally symmetric one being lower in energy. The opposite situation is encountered for the pedestal structure. Again, this finding can be traced to the particular nodal pattern of the  $\sigma$  orbitals of benzene. Depending on whether or not a member of the carbon ring lies on a nodal plane of the orbital, admixture of Si–C  $\sigma$  bond orbitals are either possible or suppressed. Therefore, different geometrical arrangements of the Si–C bonds directly lead to different adsorbate-substrate interaction induced orbital energy shifts, and thus give rise to the predicted geometry dependent differential shifts. Incidentally, tilted adsorption complexes would lead to a  $2b_{1g}$  and  $3b_{1g}$  splitting pattern very similar to that of the excluded pedestal structure.<sup>25</sup>

### E. Comparison between experiment and theory

In Sec. IV B the experimental ARUPS spectra have been discussed in detail with reference to the electronic structure of condensed multilayers of 1,4-cyclohexadiene. The photoemission data are compatible with a local  $C_{2v}$  symmetry, although in a strict sense the spectra only exhibit  $C_s(yz)$  symmetry. However, this may be rationalized by the reduced symmetry of the substrate (prior to benzene chemisorption) due to the experimentally necessary miscut of the vicinal sample. The calculated electronic structure of the energetically favored 1,4-cyclohexadiene-like  $C_6H_6/Si(001)$  model cluster has been examined in Sec. IV D including a detailed analysis of the symmetry character of each features discernible in the adsorbate-projected density of states. Several distinct differences in the symmetry-resolved PDOS for the two adsorption models, shown in Figs. 1(a) and (b), have been found. Therefore, by this combined experimental and theoretical study it is possible, as we will show, to distinguish uniquely—and independently from total energy arguments—between the proposed structure models.

A direct comparison between experiment and theory is provided by Fig. 10 where the calculated adsorbate PDOS of the butterfly cluster model is shown together with the UPS spectrum of benzene on Si(001) from Fig. 3(b). To facilitate comparison the theoretical spectrum has been shifted by 2.8 eV and stretched by a factor of 1.08 to align the lowest and highest occupied valence orbital which evolve from the  $\sigma$  system of the adsorbate (see Fig. 4). This adjustment is used to account for two aspects. First, different zero points of the energy scales have been employed: The Fermi level of the doped silicon substrate for the experimental spectrum and the absolute zero of the cluster model for the theoretical spectrum which refers to infinite separation of an electron from the adsorption complex. Second, it is well-known that differences in Kohn–Sham one-particle energies tend to underestimate valence excitation energies.

The overall agreement of the two spectra is very good. In line with the experimental results, only a very small splitting of the formerly degenerate  $2e_{1u}$  orbitals of gas-phase benzene into the 1,4-cyclohexadiene-like  $2b_{2u}$  and  $3b_{3u}$  orbitals of the adsorption complex is predicted by the calculation with the former  $b_2$ -type orbital being the lower one in energy as also suggested by the ARUPS data. The energetic ordering of the split  $2e_{2g}$  orbitals,  $4a_g(a_1)$  below  $2b_{1g}(a_2)$ ,

as well as the amount of the splitting of  $\sim 1.2$  eV are well reproduced by the calculation on the butterfly cluster model. The same holds for the symmetry equivalent  $3e_{2g}$  set, although the splitting is somewhat smaller,  $\sim 0.8$  eV. This agreement between the experimental photoemission spectrum and the one predicted for the butterfly structure is most crucial for the structure determination. As already mentioned, the alternative fourfold coordinated pedestal structure shown in Fig. 1(a) yields the opposite order of the symmetry partners:  $2b_{1g}$  below  $4a_g$  and  $3b_{1g}$  below  $6a_g$ . A tilted 1,3-cyclohexadienelike adsorption complex as proposed by Taguchi *et al.*<sup>11</sup> or other tilted configurations like the equilibrium structure found by Craig<sup>12</sup> would give rise to similar differential shifts as the fourfold coordinated adsorption complex. Based on the comparison of the experimental and theoretical data presented here we therefore conclude that on Si(001)-(2 $\times$ 1) benzene is di- $\sigma$  bonded in a 1,4-cyclohexadienelike structure to both dangling bonds of a single Si–Si dimer.

Further comparison shows that the photoemission features at 11.2 and 10.2 eV, assigned to the  $5a_g$  and  $4b_{3u}$  orbitals, correspond well in energy and symmetry character with theory. The weaker intensity for the total symmetric  $5a_g$  experimentally observed in the  $E_y D_x$  spectra is interpreted as an indication for either a broken  $xz$  symmetry of the adsorption complex or the presence of some  $b_2$  admixtures to the emission signal (see Sec. IV B). However, no such  $b_2$  features could be found in the computed PDOS in the vicinity of the  $5a_g$  peak. An energy shift of almost 2 eV with respect to the predicted energy position would be required to get the  $b_2$  symmetric  $3b_{2u}$  orbital close to the  $5a_g$  one. Such a large shift can hardly be due to many body effects, although the fact that the  $3b_{2u}$  and  $4b_{2u}$  orbitals are almost degenerate in the one-particle picture (with an energy difference of 0.05 eV only) indicates that correlation effects may be of some importance here. Thus we strongly favor the symmetry reduction due to the miscut of the vicinal Si(001) sample as explanation for the experimental findings.

The two highest occupied 1,4-cyclohexadienelike orbitals,  $1b_{3g}(b_2)$  and  $2b_{1u}(a_1)$ , which correspond to the anti-symmetric and symmetric linear combination of the two  $\pi$  bonds, are found between 4.0 and 2.3 eV experimentally and theoretically. However, the energy separation observed experimentally is about twice as large as the one calculated. On the one hand, the  $1b_{3g}$  orbital was difficult to locate in the ARUPS spectra. On the other hand, additional interactions of the  $2b_{1u}$  orbitals with laterally delocalized surface states which are beyond the scope of cluster calculations may cause an energetic shift.

The assignment of the remaining features between 8.9 and 7.9 eV which was given in Sec. IV B based on the one-particle levels calculated for gas-phase 1,4-cyclohexadiene is confirmed by the calculations on the butterfly model cluster. The  $3e_{1u}$ -derived  $5b_{3u}(b_1)$  orbital lies above the two  $b_2$ -type  $4b_{2u}$  and  $3b_{2u}$  orbitals, the latter being the energetically lower  $b_2$  orbital.

The assignment of the  $1b_{1u}$  orbital which corresponds to the former ring-shaped  $1a_{2u}$   $\pi$  orbital of gas-phase benzene is more difficult. As already mentioned this orbital splits into

several cluster orbitals upon chemisorption, among them only one (at about 7.5 eV) which still exhibits a certain localization on the adsorbate, but not strong enough to give rise to an individual peak in the total PDOS close to the  $b_1$  partner of the split  $3e_{2u}$  signal. Yet, this orbital is still rather similar to the  $1b_{1u}$  orbital of gas-phase 1,4-cyclohexadiene (Fig. 6). However, the accompanying energy stabilization of the benzene  $1a_{2u}$  orbital (about 0.5 eV) is significantly smaller than the stabilization of about 1.6 eV computed for gas-phase 1,4-cyclohexadiene (see Fig. 4) which is reasonable because silicon is far less electro-negative than hydrogen. Admixtures of this  $\pi$ -type orbital yield only small contributions to the computed PDOS of the  $C_6H_6/Si(001)$  model cluster; nevertheless they may offer an explanation for the additional photoemission intensity observed in this energy region.

## V. SUMMARY

In this combined experimental and theoretical study we have presented the first detailed analysis of the electronic structure of benzene chemisorbed on a semiconductor surface. We have shown that at saturation coverage benzene on  $Si(001)-(2 \times 1)$  is di- $\sigma$  bonded to the two dangling bonds of a single Si-Si dimer forming a 1,4-cyclohexadienelike surface complex [Fig. 1(b)]. At variance with previous semi-empirical studies,<sup>12,13</sup> our first-principles density functional cluster calculations found this butterfly structure to be more stable than the fourfold bound pedestal species shown in Fig. 1(a). Based on detailed angle-resolved photoemission data using synchrotron radiation the electronic structure and the symmetry of the adsorbate complex have been determined. By means of a dipole selection rule analysis and supported by the one-particle energy spectra calculated for the butterfly model cluster a complete assignment of the photoemission signals from benzene adsorbed on  $Si(001)-(2 \times 1)$  was given. Comparison of the symmetry-resolved photoemission spectra with symmetry classified adsorbate-projected density of states provided further arguments—independent of any total energy arguments—for the  $C_{2v}$  symmetric 1,4-cyclohexadienelike structure of the flat-lying adsorbate. In particular the energetic ordering of the formerly degenerate benzene orbitals  $2e_{2g}$  and  $3e_{2g}$  is found to depend significantly on the structure model. The orbital splittings induced in alternative structures such as the one shown in Fig. 1(a) or slightly tilted 1,3-cyclohexadiene-like structures are not compatible with the experimentally observed ordering.

## ACKNOWLEDGMENTS

We thank the BESSY crew, in particular W. Braun, for general support. This work has been supported by the Ger-

man BMBF through grant 05625WOA, by the Deutsche Forschungsgemeinschaft via SFB 338, and by the Fonds der Chemischen Industrie.

- <sup>1</sup>M. Nishijima, J. Yoshinobu, H. Tsuda, and M. Onchi, *Surf. Sci.* **192**, 383 (1987).
- <sup>2</sup>P. A. Taylor, R. M. Wallace, C. C. Cheng, W. H. Weinberg, M. J. Dresser, W. J. Choyke, and J. T. Yates, Jr., *J. Am. Chem. Soc.* **114**, 6754 (1992).
- <sup>3</sup>C. Huang, W. Widdra, X. S. Wang, and W. H. Weinberg, *J. Vac. Sci. Technol. A* **11**, 2250 (1993).
- <sup>4</sup>C. Huang, W. Widdra, and W. H. Weinberg, *Surf. Sci.* **315**, L953 (1994); **329**, 293 (1995).
- <sup>5</sup>W. Widdra, C. Huang, S. I. Yi, and W. H. Weinberg, *J. Chem. Phys.* **105**, 605 (1996).
- <sup>6</sup>U. Birkenheuer, U. Gutdeutsch, N. Rösch, A. Fink, S. Gokhale, D. Menzel, P. Trischberger, W. Widdra, and H. Koschel, *J. Chem. Phys.* (submitted).
- <sup>7</sup>R. H. Zhou, P. L. Cao, and L. Q. Lee, *Phys. Rev. B* **47**, 10601 (1993).
- <sup>8</sup>B. I. Craig and P. V. Smith, *Surf. Sci.* **276**, 174 (1992); **285**, 295 (1993).
- <sup>9</sup>Q. Liu and R. Hoffmann, *J. Am. Chem. Soc.* **117**, 4082 (1995).
- <sup>10</sup>A. J. Fisher, P. E. Blöchl, and G. A. D. Briggs, *Surf. Sci.* **374**, 298 (1997).
- <sup>11</sup>Y. Taguchi, M. Fujisawa, T. Takaoka, T. Okada, and M. Nishijima, *J. Chem. Phys.* **95**, 6870 (1991).
- <sup>12</sup>B. I. Craig, *Surf. Sci. Lett.* **280**, L279 (1993).
- <sup>13</sup>H. D. Jeong, S. Ryu, Y. S. Lee, and S. Kim, *Surf. Sci.* **344**, L1226 (1995).
- <sup>14</sup>H. A. Engelhardt, W. Bäck, D. Menzel, and H. Liebl, *Rev. Sci. Instrum.* **52**, 835 (1981); H. A. Engelhardt, A. Zartner, and D. Menzel, *Rev. Sci. Instrum.* **52**, 1161 (1981).
- <sup>15</sup>P. Feulner and D. Menzel, *J. Vac. Sci. Technol.* **17**, 662 (1980).
- <sup>16</sup>S. Gokhale, W. Widdra, A. Fink, P. Trischberger, and D. Menzel, *Rev. Sci. Instr.* (submitted).
- <sup>17</sup>H. Schlichting and D. Menzel, *Rev. Sci. Instrum.* **64**, 2013 (1993).
- <sup>18</sup>P. Jakob and D. Menzel, *Surf. Sci.* **220**, 70 (1989).
- <sup>19</sup>U. Höfer, L. Li, and T. F. Heinz, *Phys. Rev. B* **45**, 9485 (1992).
- <sup>20</sup>B. I. Dunlap and N. Rösch, *Adv. Quantum Chem.* **21**, 317 (1990).
- <sup>21</sup>A. D. Becke, *Phys. Rev. A* **38**, 3098 (1988).
- <sup>22</sup>J. P. Perdew, *Phys. Rev. B* **33**, 8822 (1986); **34**, 7406 (1986).
- <sup>23</sup>A. D. Becke, *J. Chem. Phys.* **88**, 2547 (1988).
- <sup>24</sup>P. M. W. Gill, B. G. Johnson, and J. A. Pople, *Chem. Phys. Lett.* **209**, 506 (1993).
- <sup>25</sup>U. Birkenheuer, U. Gutdeutsch, and N. Rösch, *Surf. Sci.* (submitted).
- <sup>26</sup>W. Widdra, S. Gokhale, P. Trischberger, and D. Menzel (to be published).
- <sup>27</sup>Note that the benzene nomenclature used here includes the  $C\ 1s$  core levels.
- <sup>28</sup>J. H. D. Eland, *Photoelectron Spectroscopy* (Butterworths, London 1974), p. 97.
- <sup>29</sup>W. L. Jorgensen and L. Salem, *The organic chemist's book of orbitals* (Academic, New York, 1993).
- <sup>30</sup>P. Krüger and J. Pollmann, *Phys. Rev. B* **38**, 10578 (1988).
- <sup>31</sup>W. Widdra, S. Gokhale, P. Trischberger, and D. Menzel (unpublished).
- <sup>32</sup>J. L. Gland and G. A. Somorjai, *Surf. Sci.* **38**, 157 (1973).
- <sup>33</sup>W. Huber, M. Weinelt, P. Zebisch, and H.-P. Steinrück, *Surf. Sci.* **253**, 72 (1991).
- <sup>34</sup>L. S. O. Johansson, R. I. G. Uhrberg, R. Lindsay, P. L. Wincott, and G. Thornton, *Phys. Rev. B* **42**, 9534 (1990).
- <sup>35</sup>M. Weinelt, W. Huber, P. Zebisch, H.-P. Steinrück, M. Pabst, and N. Rösch, *Surf. Sci.* **271**, 539 (1992).
- <sup>36</sup>M. Weinelt, W. Huber, P. Zebisch, H.-P. Steinrück, P. Ulbricht, U. Birkenheuer, J. C. Boettger, and N. Rösch, *J. Chem. Phys.* **102**, 9709 (1995).
- <sup>37</sup>U. Gutdeutsch, U. Birkenheuer, E. Bertel, J. Cramer, J. C. Boettger, and N. Rösch, *Surf. Sci.* **345**, 331 (1996).